Available online at www.sciencedirect.com
ScienceDirect
Trans. Nonferrous Met. Soc. China 28(2018) 879−889
Transactions of Nonferrous Metals Society of China
www.tnmsc.cn

Solidification behavior of 6061 wrought aluminum alloy during rheo-diecasting process with self-inoculation method

Ming LI[1], Yuan-dong LI[1,2], Hong-qiang ZHENG[1], Xiao-feng HUANG[1,2], Ti-jun CHEN[1,2], Ying MA[1,2]

1. State Key Laboratory of Advanced Processing and Recycling of Nonferrous Metals, Lanzhou University of Technology, Lanzhou 730050, China;
2. Key Laboratory of Non-ferrous Metal Alloys, Ministry of Education, Lanzhou University of Technology, Lanzhou 730050, China

Received 22 December 2016; accepted 2 August 2017

Abstract: The semisolid slurry of the 6061 wrought aluminum alloy was prepared by the self-inoculation method (SIM). The effects of the isothermal holding parameters on microstructures of rheo-diecastings were investigated, and the solidification behavior of 6061 wrought aluminum alloy during the rheo-diecasting process was analyzed using OM, SEM, EDS and EBSD. The results indicate that the isothermal holding process during slurry preparation has great effect on primary α(Al) particles (α_1), but has little effect on the microstructure of secondary solidification in the process of thin-walled rheo-diecasting. Nucleation is expected to take place in the entire remaining liquid when the remaining liquid fills the die cavity, and the secondary solidification particles (α_2) are formed after the process of stable growth, unstable growth and merging. The solute concentration of remaining liquid is higher than that of the original alloy due to the existence of α_1 particles, hence the contents of Mg and Si in α_2 particles are higher than those in α_1 particles.

Key words: 6061 wrought aluminum alloy; solidification behavior; primary particle; secondary particle; rheo-diecasting

1 Introduction

The wrought alloys are widely used in aerospace, automotive industry and national defense and military industry due to their superiority, such as heat treatment strengthening and high performance [1−4]. However, their poor casting performance makes them difficult to be produced by permanent mold casting, low pressure casting and high pressure casting [5]. The general forming processes for wrought alloy are forging, rolling and extrusion. But they can not be used to produce complex shaped components. Hence, the direct forming method of the wrought alloy has become a new focus [6,7]. While semisolid forming has opened up a new way for the near net forming of wrought alloy. In the semisolid forming process, remaining liquid phase of alloy can be connected with each other due to the existence of non dendritic solidification structures in the semisolid slurry, which can effectively reduce or eliminate the solidification shrinkage. Therefore, the semisolid forming technology can obtain the products with free hole-class defects in theory [8−12], which is suitable for the forming requirements of wrought alloy.

Theoretically, the wrought aluminum alloy is suitable for semisolid forming due to its wide temperature range of solidus and liquidus. The previous researches on semisolid forming of wrought aluminum alloy are mainly focused on thixoforming because of its high temperature sensitivity [13−15]. But recently, rheoforming has aroused much attention due to its low cost and high productivity compared with thixoforming. The rheoforming of wrought aluminum alloy has been achieved by combining different slurry preparation methods with rolling, extrusion and diecasting. LI et al [16] prepared 2024 wrought aluminum alloy semisolid slurry by self-inoculation method (SIM) and produced the rheo-diecastings with primary phase uniformly distributed. ZHAO et al [17] proposed a melt treatment with a vibrating cooling slope and a semisolid rolling process to produce an AZ61 alloy strip. JIN et al [18] prepared the semisolid slurry of 6061 wrought aluminum alloy with electromagnetic stirring, and directly used forging technique to form thin plate parts. CURLE [19]

Foundation item: Project (51464031) supported by the National Natural Science Foundation of China
Corresponding author: Yuan-dong LI; Tel: +86-931-2976795; E-mail: liyd_lut@163.com
DOI: 10.1016/S1003-6326(18)64721-1

successfully realized the rheo-diecasting to form commercial wrought aluminum alloy by combining Council for Scientific and Industrial Research-Rheocasting System (CSIR-RCS) technology with high pressure die casting, and the yield strength of the alloys is close to the level of the forging.

In this work, the slurry of 6061 wrought aluminum alloy was prepared by SIM [20], and the SIM process was integrated with high pressure die casting (HPDC) machine to produce thin-walled parts. The effects of different isothermal holding parameters on microstructures and solidification behavior of 6061 wrought aluminum alloy were studied to provide a theoretic basis for the optimization of process parameters and its application.

2 Experimental

2.1 Preparation of self-inoculants

The 6061 wrought aluminum alloy was used as the raw material (actual composition is given in Table 1). The molten alloy was degassed by C_2Cl_6 (1% (mass fraction) of alloy) at 730 °C, then cooled to 700 °C and poured into a metal mold to obtain the metal bars with the sizes of *d*15 mm × 150 mm. Then, the bars were machined into small particles with sizes of about 5 mm × 5 mm × 5 mm.

Table 1 Chemical composition of 6061 aluminum alloy (mass fraction, %)

Mg	Si	Cu	Cr	Mn	Zn	Ti	Fe	Al
1.02	0.73	0.3	0.12	0.09	0.11	0.04	0.15	Bal.

2.2 Slurry preparation and rheo-diecasting

Figure 1 shows the schematic diagram of slurry preparation by SIM. The fluid director was inclined at 45° with a length of 500 mm. The 6061 wrought alloy was melted and degassed. The melt temperature was adjusted to 730 °C and 5% (mass fraction of the melt) inoculants were added into the melt, followed by hand stirring the melt with a iron bar quickly to make them dissolved. Then, the mixed melt was collected through fluid director to the slurry collector to obtain semisolid slurry. Finally, the prepared slurry was isothermally held for a certain time (0, 3, 5 and 10 min, respectively) at 640 °C. The prepared slurry was employed to the rheo-diecasting experiment of thin-walled part with DAK−450 die casting machine. The dies were preheated to 200 °C by hot circulating oil and shot chamber was preheated to 300 °C. The injection rate was 1.2 m/s with pressure of 160 MPa. Real diagram of die casting is shown in Fig. 2 with the diameter of 200 mm and the wall thickness of 2 mm.

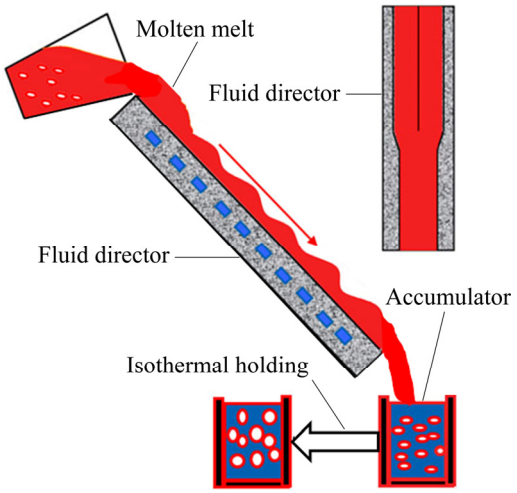

Fig. 1 Schematic diagram of slurry preparation process of SIM

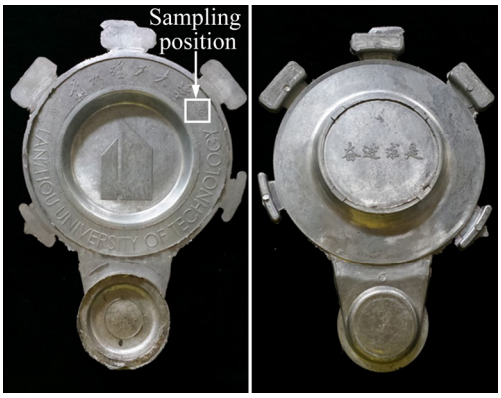

Fig. 2 Die casting component and sampling position

2.3 Microstructure observation and quantitative analysis

Forming process and solidification behavior of rheo-diecasting were studied by microstructures of certain positions (as shown in Fig. 2). The specimens were prepared by the standard technique of grinding with SiC abrasive paper and polishing with an Al_3O_2 suspension solution, followed by etching in Keller reagent (2 mL HF + 3 mL HCl + 5 mL HNO_3 + 190 mL H_2O). The optical microscopy (OM) was carried out to observe the microstructures of primary particles, and the average particle sizes ($D=(4A/\pi)^{1/2}$, where A is area of the particle) and shape factors ($F=P^2/(4\pi A)$, where P is the perimeter of particle) of primary particles were measured using image analysis software Image-Proplus6.0. The FEG450 scanning electron microscopy (SEM) was carried out, equipped with an energy dispersive spectroscopy (EDS) and operated at an accelerating voltage of 3−20 kV to observe the morphologies of secondary particles. Then, the specimens were etched using electrolytic etching method in perchloric acid alcohol solution (with the volume ratio of 1:9, the voltage of 18 V and the soaking time of 30−40 s) to

observe the distribution difference of secondary particles between isothermal holding specimen and non-isothermal holding specimen by electron back-scattered diffractometry (EBSD).

The differential scanning calorimetry (DSC) curve of 6061 wrought aluminum alloy is shown in Fig. 3. It can be seen that the solidus and liquidus of the alloy are 586.9 and 651.3 °C, respectively, presenting the wide solid−liquid range, which is suitable for semisolid processing.

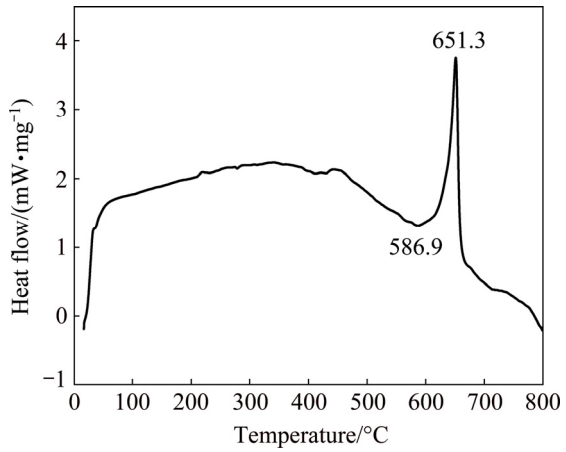

Fig. 3 Differential scanning calorimetry (DSC) curve of 6061 wrought aluminum alloy

The suitable range of solid fraction for semisolid metal forming is 30%−50%. Based on the calculation of the Al−Mg alloy phase diagram and Schiel formula, the relationship between temperature and solid fraction of 6061 wrought aluminum alloy is obtained, as shown in Fig. 4. The corresponding temperature processing window for semisolid processing is 10.3 °C (ΔT_{TPW}= 645.5 °C − 635.2 °C =10.3 °C). After comprehensive consideration, 640 °C is chosen as the isothermal holding temperature of 6061 wrought aluminum alloy.

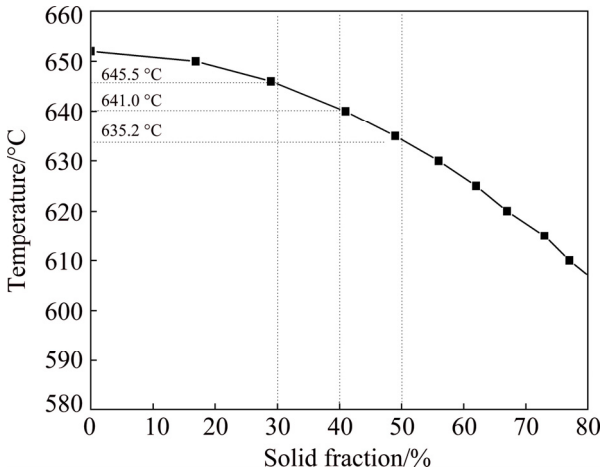

Fig. 4 Temperature processing window of 6061 wrought aluminum alloy

3 Results

3.1 Microstructures of 6061 wrought aluminum alloy in different forming ways

Figure 5 shows the microstructures of 6061 wrought aluminum alloy in different forming ways. It can be seen that morphologies of primary α(Al) are mainly composed of coarse dendrites in traditional permanent mold casting (as shown in Fig. 5(a)). While the microstructures of semisolid permanent mold casting mainly consist of spherical and rose-like primary α(Al), which are surrounded by fine dendrites formed during the solidification of remaining liquid (as shown in Fig. 5(b)). In the microstructure of semisolid rheo-diecasting by SIM (as shown in Fig. 5(c)), the near spherical α(Al) particles are formed during the process of slurry

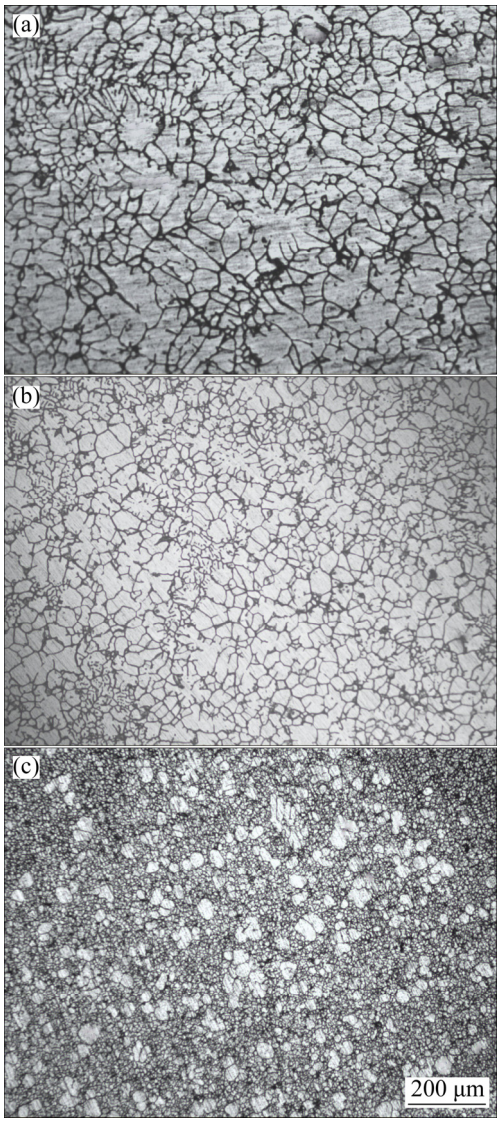

Fig. 5 Microstructures of 6061 alloy in different forming ways: (a) Traditional permanent mold casting; (b) Semisolid permanent mold casting by SIM; (c) Semisolid rheo-diecasting by SIM

preparation, and the fine secondary solidification particles are formed in the filling process of the remaining liquid. The secondary solidification particles are too fine to show clear morphologies due to the fast cooling rate during the rheo-diecasting process. It is obviously shown that high pressure die casting integrated with the semisolid slurry prepared by SIM can obtain ideal semisolid microstructure with spherical and uniformly distributed primary α(Al).

3.2 Effect of isothermal holding time on primary particles of rheo-diecastings

The microstructures of 6061 wrought aluminum alloy produced by rheo-diecasting technology with different isothermal holding time of the semisolid slurry are shown in Fig. 6. It can be clearly observed from the microstructure of rheo-diecasting without isothermal holding that the primary α(Al) (α_1) particles present fine structures with some dendritic fragments. After the isothermal holding process, the size of primary particles gradually increases and becomes spherical (as shown in Figs. 6(b) and (c)). With the isothermal holding time further increasing, the merging phenomenon occurs, leading to the irregular growth of the primary particles (Fig. 6(d)). The average grain sizes and shape factors are measured, as shown in Fig. 7. In the microstructure of rheo-diecasting without isothermal holding, the average grain size of α_1 particles is 35 μm, and the corresponding roundness is 1.6. When the isothermal holding time is 3 and 5 min, the average grain sizes of α_1 particles are 56 and 76 μm, respectively, with the corresponding roundness of 1.42 and 1.25, respectively. The average grain size of α_1 particles increases to 101 μm with the corresponding roundness of 1.45 when the isothermal holding time increases to 10 min.

Figure 8 shows the linear fitting of the growth of primary particles with different isothermal holding time. It is evident combined with Fig. 7 that primary particles gradually grow and spheroidize in the early stage of isothermal holding process, and the growth rate of the primary particles in the isothermal holding process conforms to the dynamic equation of $D_t^3-D_0^3=Kt$ [21] (where D_0 is the primary solid particle diameter without isothermal holding, D_t is the average particle size after isothermal holding for t, and K is the coarsening rate constant). After comprehensive analysis, the suitable isothermal holding time of semisolid slurry for the rheo-diecasting process of 6061 wrought aluminum alloy is 5 min.

3.3 Effect of isothermal holding time on secondary particles of rheo-diecasting

Figure 9 shows the morphologies of secondary particles (α_2) in rheo-diecastings with different isothermal holding time. It can be clearly observed that the sizes of secondary particles are smaller than those of primary particles. The α_2 particles, which are connected with each other, are nearly spherical and in rose-like

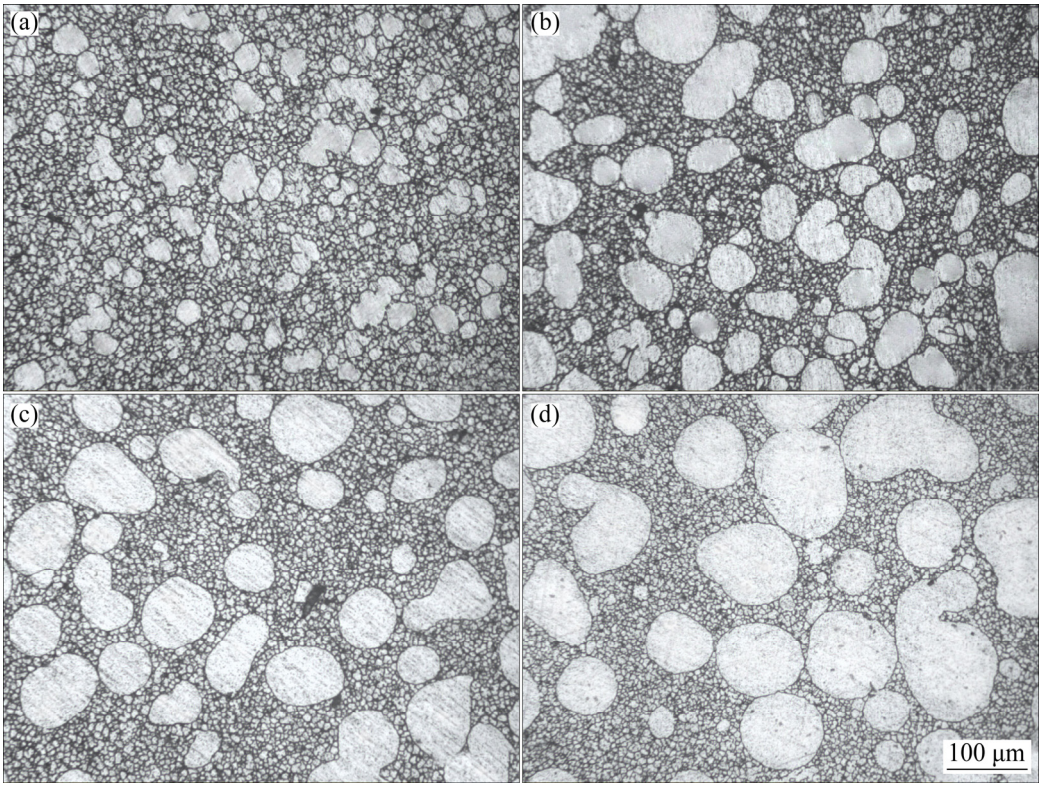

Fig. 6 Microstructures of 6061 alloy rheo-diecast by SIM at different holding time: (a) 0 min; (b) 3 min; (c) 5 min; (d) 10 min

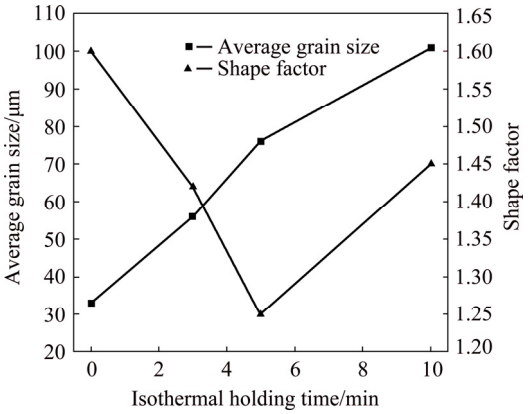

Fig. 7 Changes of primary particle size and shape factor with isothermal holding time

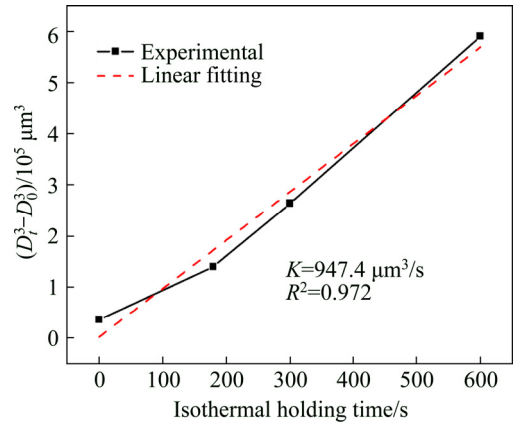

Fig. 8 Linear fitting of growth of primary particles of 6061 alloy with isothermal holding time at 640 °C

shape with different holding time. Meanwhile, the segregation of eutectic structures has not been observed in the microstructures. The particle sizes and shape factors of α_2 particles are measured, as shown in Fig. 10. It can be seen from Fig. 10 that the average particle sizes of α_2 particles with different holding time fluctuate in the range of 11.7−11.9 μm, while the corresponding shape factors change from 1.35 to 1.41, indicating the little effects of isothermal holding time on secondary solidification microstructures of thin-walled rheo-diecastings.

The EBSD analysis is employed to further investigate the effect of isothermal holding process on the microstructures of secondary solidification. The measured results (as shown in Fig. 11) are achieved by analyzing the sample without isothermal holding (Fig. 11(a)) and the sample held for 5 min (Fig. 11(b)). It can be observed that the EBSD microstructures of secondary solidification for two samples have no obvious difference (Figs. 11(a) and (b)). And the statistics of misorientation angles have no obvious change (Figs. 11(c) and (d)). Furthermore, the distribution of circle equivalent diameters of two samples shows the same results that the size of secondary particles is mainly distributed less than 10 μm (as shown in Figs. 11(e) and (f)). Hence, the different isothermal holding processes have no obvious effect on secondary solidification microstructures of thin-walled rheo-diecastings.

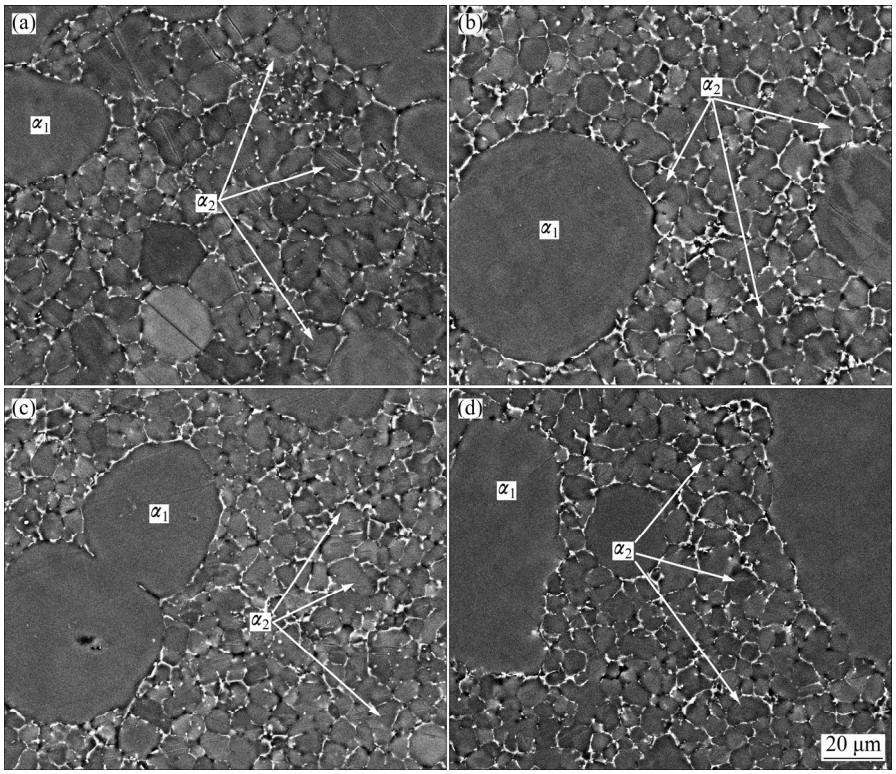

Fig. 9 SEM images of 6061 alloy rheo-diecast by SIM at different holding time: (a) 0 min; (b) 3 min; (c) 5 min; (d) 10 min

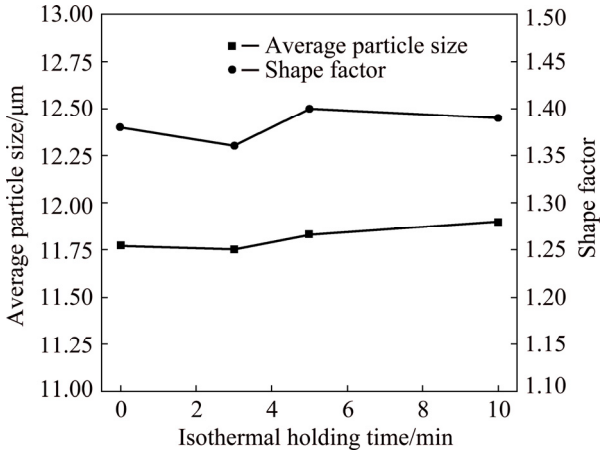

Fig. 10 Changes of secondary particle size and shape factor with isothermal holding time

4 Discussion

4.1 Microstructure analysis of semisolid slurry prepared by SIM

When the semisolid slurry of 6061 wrought aluminum alloy is prepared by SIM, the temperature of 6061 wrought aluminum alloy melt will be decreased rapidly after adding the self-inoculants. As a result, there will be a large number of high melting points and "large sized atomic clusters" in the local position of the melt, which will be used as the nucleation sites. On the other hand, the addition of self-inoculants can be regarded as the addition of heterogeneous nucleation site in the melt, making the nucleation rate increase, which is called the process of primary inoculation. When the melt flows

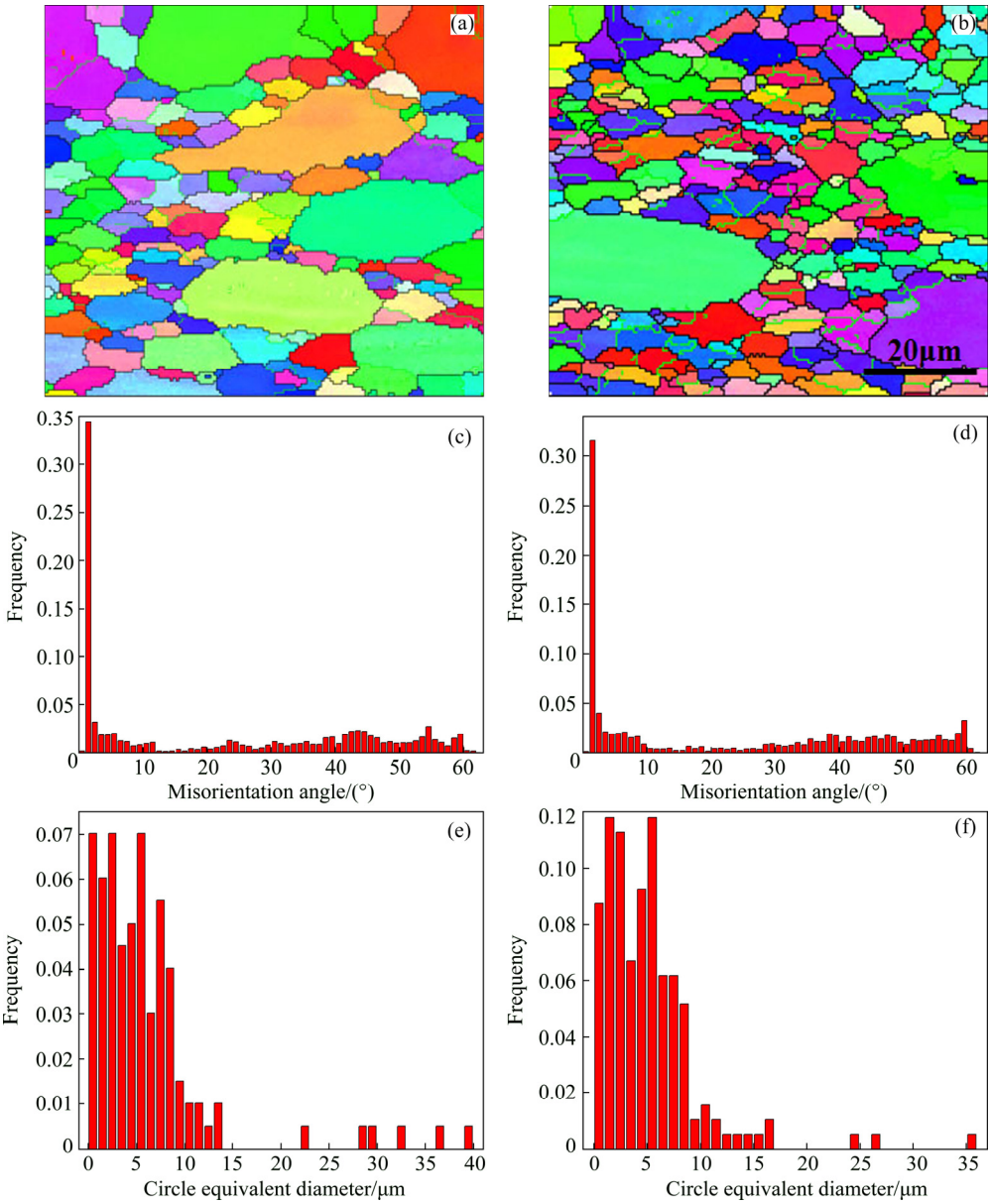

Fig. 11 EBSD analysis results and relevant statistics of samples: (a, c, e) Without isothermal holding; (b, d, f) Isothermal holding for 5 min

through the fluid director, the solidified shell is formed rapidly under the chilling of director surface due to the low temperature of the director. Subsequently, free grains and dendritic fragments are formed and involved in the melt when the subsequent melt scours and shears the solidified shell strongly, and finally evolve into rose-shape and fine dendritic primary particles. During this process, the temperature of the melt decreases and the undercooling of the semisolid slurry increases due to the heat transfer and convection, leading to the dendritic primary particles survived, which is called the process of secondary inoculation. At the end of the director, turbulence occurs when two streams of the melt are converged, which promotes thermal field and concentration field of the melt to be homogeneous. The metal mold structure of semisolid slurry and the microstructures of solidified shell at the inlet and outlet of the director have been observed, and the results are shown in Fig. 12. The microstructure of solidified shell at the inlet of the director is composed of large dendrites. When the melt passes through the director, the microstructure of solidified shell at the outlet of the director is composed of rose-like crystals. Finally, when the slurry is collected in the accumulator, the microstructure exhibits the fine equiaxed crystals due to the fusing of rose-like crystals. Hence, the semisolid slurry of 6061 wrought aluminum alloy can be prepared by SIM. Compared with coarse dendrites in traditional casting, the primary α(Al) particles in semisolid structures are uniformly distributed with fine and spherical morphologies.

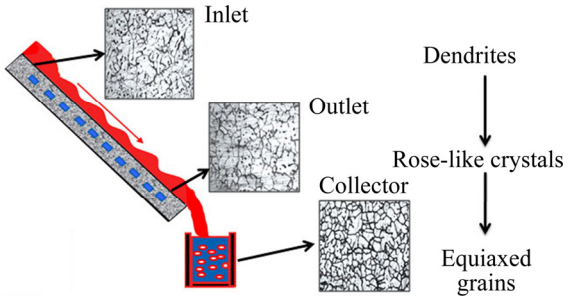

Fig. 12 Microstructural evolution of 6061wrought aluminum alloy during secondary inoculation process

4.2 Effect of isothermal holding process on α_1 particles

Self-inoculation rheo-diecasting is a novel rheo-diecasting process combining slurry preparation process by SIM with HPDC. And the preparation of the fine semisolid slurry is the precondition to ensure the high quality and integrity of the die castings. When the slurry is prepared without isothermal holding, there are amount of dendritic fragments and high melting point particles inside the melt. After collecting in the accumulator, the convection will be generated when two streams of the melt are converged, making the tips of dendritic fragments passivated. During isothermal holding process, the dendrite fragments are fused due to enrichment of the root solute, which leads to the formation of single irregular particles, and the tips of these irregular particles are melted. At the same time, the increased amount of particles makes the interfacial energy increase. Primary particles, as the substrates to absorb solute atoms from liquid phase, are rounded and spherical under the influence of the driving force, and the interfacial energy can be reduced as far as possible. Consequently, primary particles are increased and spherical with the extension of isothermal holding time. However, different sizes of original dendritic fragments result in different diameters of spherical primary particles after isothermal holding for a short time. The solute concentration of liquid phase around smaller particles is lower than that around larger particles. With the further extension of the holding time, Mg and Si elements continue to diffuse from large particles to small particles, while the Al elements have the opposite diffusion path. As a result, large particles become larger and small particles become smaller, even melted and disappeared, which is called Oswald ripening [22]. The “8” shaped and spindle-like structures are formed as the intensification of merge phenomenon in the late stage of isothermal holding process. When the two particles with large difference in sizes are incorporated and grow into a new shape, the new particle will eventually be spherical under the driving force of the interfacial energy reduced. But when the two particles with same size are merged into a new particle, it will be very difficult to be spherical, and eventually grow into “8” or “shuttle” shaped clusters. According to the previous experimental study, the suitable isothermal holding time of the slurry for rheological forming of 6061 wrought aluminum alloy is 5 min. In this condition, the sizes of α_1 particles are not very large and the shape factor of particles is the best.

4.3 Secondary solidification behavior of thin-walled rheo-diecasting

The secondary solidification starts when the semisolid slurry leaves holding furnace. When the slurry is injected into the die cavity, there are two processes in the remaining liquid: nucleation and growth. The thickness of the forming part used in the experiment is 2 mm. During the filling process, the semisolid slurry contacts with the cold mould under high pressure, which can provide a large supercooling. The nucleation rate is expressed as follows [23]:

$$N = K\exp(\frac{-\Delta G}{kT})\cdot\exp(\frac{-Q}{kT}) \quad (1)$$

where K is a constant, ΔG is the nucleation energy, Q is

the diffusion activation energy of atoms across the liquid/solid interface, k is the Boltzmann constant, and T is thermodynamic temperature. For most of the alloy melt, the nucleation rate is increased significantly when the value of relative supercooling is $(0.15-0.25)T_m$ (T_m is the melting temperature of alloy), which is called the "explosive" nucleation. The melting temperature of 6061 wrought aluminum alloy used in this experiment is about 650 °C, while the dies are preheated to 200 °C and the pouring temperature of alloy is 640 °C, which provides a large enough relative supercooling for "explosive" nucleation. Therefore, nucleation occurs throughout the whole remaining liquid in the thin-walled positions. Furthermore, the nuclei can survive due to high cooling rate provided by die cavity.

In the process of secondary solidification, Al phases crystallizing in remaining liquid grow, attaching α_1 particles initially [24], while the explosive nucleus grow into fine spherical particles stably, which is called stable growth. With the solidification process continuing, α_2 particles grow unstably after reaching their critical size of stable growth. Within the limitation of solidification region, the α_2 particles present the near spherical shape and merge into irregular particles (as shown in Fig. 13). In addition, the attaching growth around α_1 particles is continued and at the same time α_2 particles grow. As a result, the temperature fluctuations occur in the front of the interface, and then the perturbation is generated ahead of the interface of growing crystals. During the solidification process, the stably enriched layer of solute atoms is generated in the liquid phase ahead of the interface, which will lead to the formation of "constitutional undercooling" zone. At this time, the liquid phase in "constitutional undercooling" zone is in a quasi steady state, meaning that there is a driving force promoting perturbation to grow. Consequently, the temperature gradient and the concentration gradient in the liquid phase are increased at the tip of the solid/liquid interface, which will also lead to the increase of liquidus gradient. Finally, the "constitutional undercooling" zone will survive, making the perturbation around α_1 particles gradually grow into the microstructures of "cellulation" or "dentation" (as shown in Fig. 13). But the "cellulation" or "dentation" structure will be finally preserved due to the rapid cooling and limitation of α_2 particles.

The Mullins–Sekerka instability theory [25] pointed out that a spherical crystal growing from a melt is morphologically unstable when its size exceeds a critical value R_c:

$$R_c=\frac{2\Gamma(7+4k_s/k_l)}{[(T_m-T_\infty)/T_m]}=\frac{2(\gamma_{sl}/L_v)(7+4k_s/k_l)}{\Delta T/T_m} \quad (2)$$

where T_m and T are the melting point and melt temperature, respectively; k_s and k_l are thermal conductivities of liquid and solid Al at the melting point temperature; γ_{sl} is the interfacial energy at the solid/liquid interface; L_v is the latent heat of fusion per unit volume of the solid. Substituting the thermophysical values of pure aluminum [26] into the above equation gives

$$R_c=\frac{5.12}{\Delta T} \quad (3)$$

It can be seen that the critical value, R_c, for stable spherical growth is sensitive to the undercooling, ΔT. It is difficult to directly measure the undercooling achieved by the α(Al) (α_2) growing from the alloy melt inside the die cavity. According to the existed research [27,28], assuming a similar undercooling level of 1−2 K, in the secondary solidification process, Mullins–Sekerka stability theory, Eq. (3), tells us that α(Al) spherical crystals will grow stably until their size is 5.12−10.24 μm or larger. Actually, the undercooling of thin-walled diecasting is larger than above assumption, meaning that the α_2 particles have grown unstably when their size arrives to 5.12 μm. In this work, the measured sizes of secondary particles of 6061 wrought aluminum alloy at different holding parameters are in the range of 11.7−11.9 μm, indicating that the α_2 particles are actually unstable. Moreover, the measured sizes of α_2 particles are more than twice of critical value, indicating that the merging phenomena have occurred among α_2 particles due to the enough nucleus and limited region during the solidification of remaining liquid. And the relatively large shape factor (1.35−1.41) can further prove the unstable growth of α_2 particles.

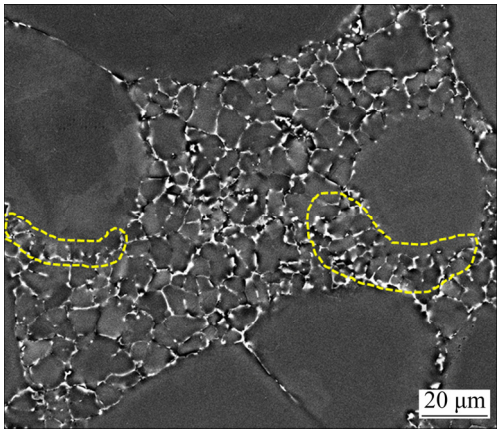

Fig. 13 Unstable growth of particles

4.4 EDS analysis

In order to illustrate the difference of element distribution between primary particles and secondary particles, the EDS analysis of α_1 and α_2 particles was

carried out. The results are given in Table 2. It can be achieved that no matter holding or not, the Mg and Si contents in both α_1 and α_2 particles are relatively stable, indicating the stable solute concentration during the isothermal holding process, which is the main reason for the formation of same solidification microstructures of remaining liquid with different isothermal holding parameters. Meanwhile, different solute concentrations between α_1 and α_2 particles with the same parameter illustrate the different solidification stages of primary solidification and secondary solidification.

Figure 14 shows the elements distribution of Mg, Si and Cu. It can be seen that Mg and Si are mainly distributed in the eutectic structure of intergranular regions, and only small amounts are distributed in α_1 and α_2 particles. Cu is only enriched in the eutectic structure of intergranular regions due to its little original amount. Other elements such as Cr, Mn, Zn, Ti and Fe have not been detected. The results of Fig. 14 are consistent with the measured element contents given in Table 2.

The EDS data of Table 2 and Fig. 14 show the different processes between primary solidification and secondary solidification. The main elements of 6061 wrought aluminum alloy are Al, Mg, Si and Cu. According to Fig. 4, the solid fraction of 6061 wrought aluminum alloy at 640 °C is about 40%, and theoretical compositions of original alloy and remaining liquid are measured by thermodynamic calculation software, Pandat, as given in Table 3. The results show that the contents of Mg, Si and Cu in remaining liquid are higher than those of the original alloy. The different contents of Mg in α_1 and α_2 particles (as shown in Table 2 and Fig. 15) indicate that the α_1 particles are formed in primary solidification process, while the α_2 particles are

Table 2 Element contents in α_1 and α_2 particles

Isothermal holding time/min	Primary particle α_1				Secondary particle α_2			
	w(Al)/%	w(Mg)/%	w(Si)/%	w(Cu)/%	w(Al)/%	w(Mg)/%	w(Si)/%	w(Cu)/%
0	99.4	0.4	0.2	0	99.1	0.6	0.3	0
3	99.4	0.4	0.2	0	99.0	0.6	0.4	0
5	99.3	0.4	0.3	0	98.9	0.7	0.4	0
10	99.3	0.4	0.3	0	98.8	0.8	0.4	0

The spot scanning positions of α_1 and α_2 particles are in the center of particles.

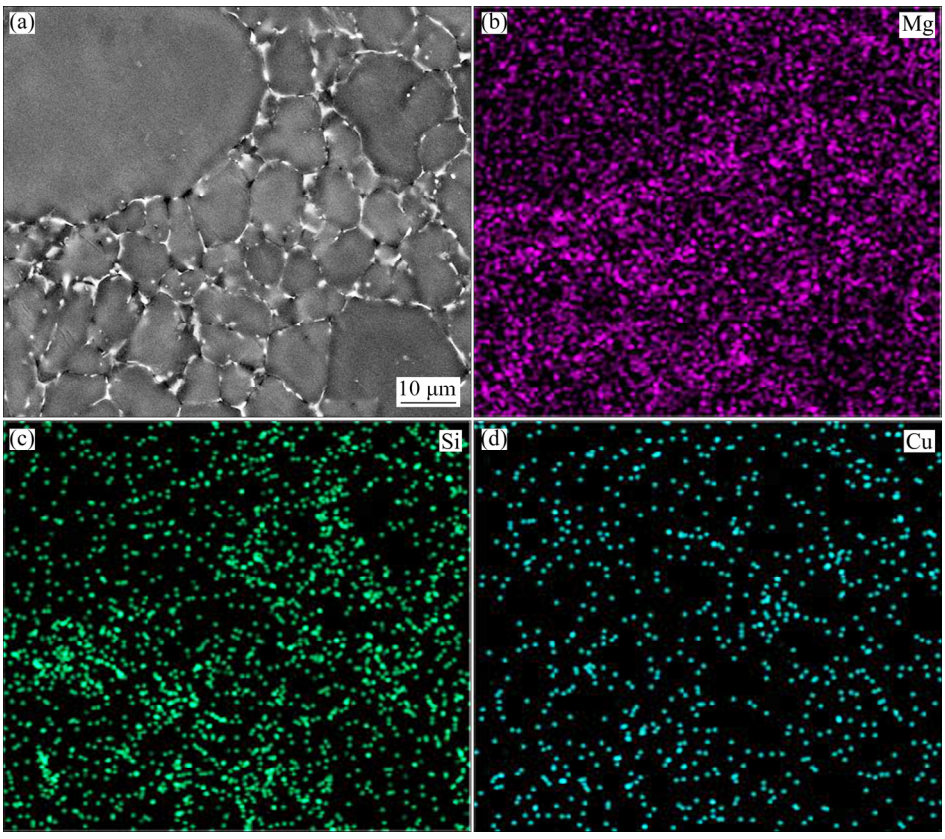

Fig. 14 Elemental distributions of 6061 wrought aluminum alloy produced by rheo-diecasting: (a) Morphology; (b) Mg; (c) Si; (d) Cu

Table 3 Theoretical compositions of original alloy and remaining liquid (mass fraction, %)

Location	Al	Mg	Si	Cu
Original alloy	0.980	0.010	0.007	0.003
Remaining liquid	0.969	0.015	0.011	0.005

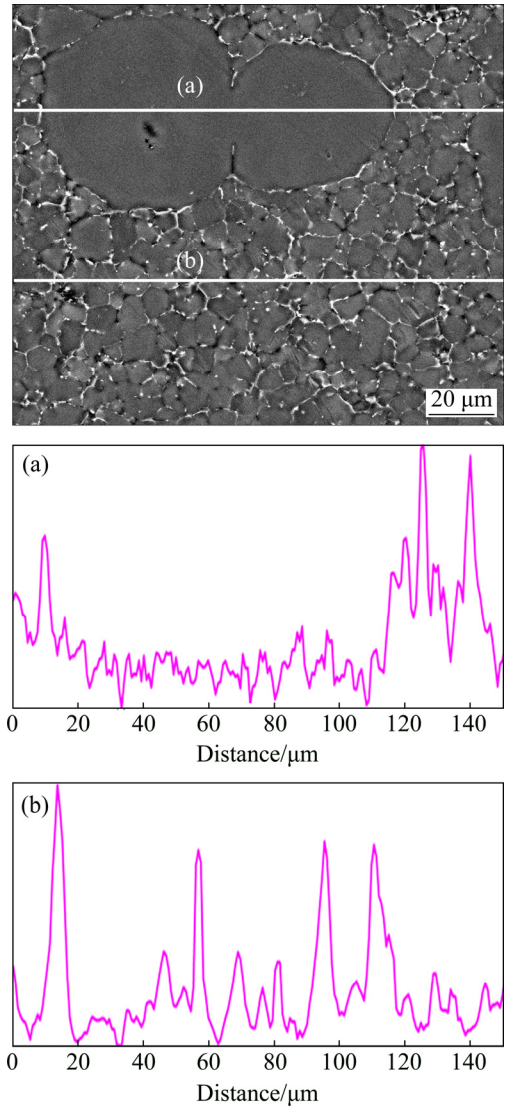

Fig. 15 EDS analysis results of Mg contents in primary particles (a) and secondary particles (b)

formed in secondary solidification process due to the high fraction of remaining liquid. During the rheo-diecasting process, Mg enriched ahead of the interfaces has no time to diffuse and finally reserves in α_2 particles due to high cooling rate. Furthermore, in the solidification process of remaining liquid, primary particles (α_1), as substrates absorbing Al atoms crystallize from remaining liquid, have partially grown. As the result, Mg content has the tendency of slow increase at the edge of α_1 particles (as shown in Fig. 15(a)).

5 Conclusions

1) The dendritic structures produced by traditional casting can be effectively modified by SIM to obtain the microstructures with fine equiaxed and near spherical primary particles. The primary α(Al) particles of 6061 wrought aluminum alloy are round and distributed uniformly when the components are produced by rheo-diecasting.

2) The isothermal holding process during slurry preparation by SIM has great effect on primary α(Al) particles (α_1), but has little effect on the microstructure of secondary solidification in the process of thin-walled rheo-diecasting. The suitable isothermal holding time of semisolid slurry for rheo-diecasting of 6061 wrought aluminum alloy is 5 min.

3) When the remaining liquid fills die cavity, due to the large cooling rate provided by metallic dies, nucleation is expected to take place in the entire remaining liquid, and the secondary solidification particles (α_2) are formed after the process of stable growth, unstable growth and merging. On the effect of constitutional undercooling, in the primary (α_1) particles, unstable growth phenomenon will appear.

4) The solute concentration of remaining liquid is higher than that of the original alloy due to the existence of α_1 particles, hence the contents of Mg and Si in α_1 particles are higher than those in α_2 particles.

References

[1] ZHANG Pei-wu, XIA Wei, LIU Yin, ZHANG Wei-wen, CHEN Wei-ping. The research of wrought magnesium alloy forming technology and its application [J]. Materials Review, 2005, 19(7): 82−85. (in Chinese)

[2] CHEN Zhen-hua. Wrought magnesium alloy [M]. Beijing: Chemical Industry Press, 2005. (in Chinese)

[3] PAN Fu-sheng, ZHANG Ding-fei. Aluminum alloy and its application [M]. Beijing: Chemical Industry Press, 2006. (in Chinese)

[4] WU Gong, YAO Liang-jun, LI Zheng-xia, PENG Ru-qing, ZHAO Zu-de. Handbook of aluminium and aluminium alloys [M]. Beijing: Science Press, 1994. (in Chinese)

[5] QI Pei-xiang. Squeezing casting for wrought aluminum alloy [J]. Special Casting and Nonferrous Alloy, 2008, 28(10): 769−772. (in Chinese)

[6] HU K, PHILLION A B, MAIJER D M, COCKCROFT S L. Constitutive behavior of as-cast magnesium alloy Mg−Al3−Zn1 in the semi-solid state [J]. Scripta, 2009, 60(6): 427−430.

[7] KIM S K, YOON Y Y, JO H H. Novel thixoextrusion process for Al wrought alloys [J]. Journal of Materials Processing Technology, 2007, 187−188(12): 354−357.

[8] FLEMINGS M C. Behavior of metal alloys in the semi-solid state [J]. Metallurgical and Materials Transactions B, 1991, 22(5): 957−981.

[9] LUO Shou-jing, JIANG Yong-zheng, LI Yuan-fa, SHAN Wei-wei. Recognition of semi-solid metal forming technologies [J]. Special Casting and Nonferrous Alloy, 2012, 32(7): 603−607. (in Chinese)

[10] ESKIN D G, KATGERMAN S L. Mechanical properties in the semi-solid state and hot tearing of aluminum alloys [J]. Progress in Materials Science, 2004, 49(5): 629−711.
[11] XU Jun, ZHANG Zhi-feng. Research progress of semisolid processing technology [J]. Journal of Harbin University of Science and Technology, 2013, 18(2): 1−6. (in Chinese)
[12] ZHAO Jun-wen, WU Shu-sen. Microstructure and mechanical properties of rheo-diecast A390 alloy [J]. Transactions of Nonferrous Metals Society of China, 2010, 20(S3): s754−s757.
[13] WANG Zhi-bo, LIU Chang-ming, HAN Zhao-tang. Structure evolution characteristics of wrought aluminum alloy 7050 in the process of semi-solid forging and its mechanical properties [J]. Aluminum Fabrication, 2008(1): 16−20. (in Chinese).
[14] LU Gui-min, DONG Jie, CUI Jian-zhong, WANG Ping. Study on the reheating and thixoforming of 7075 aluminum alloy cast by liquidus semi-continuous casting [J]. Acta Metallurgica Sinica, 2001, 31(11): 1184−1188.
[15] WANG Shun-cheng, LI Yuan-yuan, CHEN Wei-ping, ZHENG Xiao-ping. Microstructure evolution of semi-solid 2024 alloy during two-step reheating process [J]. Transactions of Nonferrous Metals Society of China, 2008, 18(4): 784−788.
[16] LI Yan-lei, LI Yuan-dong, LI Chun, WU Hui-hui. Microstructure characteristics and solidification behavior of wrought aluminum alloy 2024 rheo-diecast with self-inoculation method [J]. China Foundry, 2012, 9(4): 328−336.
[17] ZHAO Zhan-yong, GUAN Ren-guo, WANG Xiang, LI Yang, DONG Lei, LEE C S, LIU Chun-ming. Microstructure formation mechanism and properties of AZ61 alloy processed by melt treatment with vibrating cooling slope and semisolid rolling [J]. Metals and Materials International, 2013, 19(5): 1063−1067.
[18] JIN C K, BOLOURI A, KANG C G. Mechanical properties and microstructure of thin plates of A6061 wrought aluminum alloy using rheology forging process with electromagnetic stirring [J]. Metallurgical and Materials Transactions B, 2013, 45(3): 1068−1080.
[19] CURLE U A. Semi-solid near-net shape rheocasting of heat treatable wrought aluminum alloy [J]. Transactions of Nonferrous Metals Society of China, 2010, 20(9): 1719−1724.
[20] LI Yuan-dong, YANG Jian, MA Ying, QU Jun-feng, ZHANG Peng. Effect of pouring temperature on AM60 Mg alloy semi-solid slurry prepared by self-inoculation method (I) [J]. Transactions of Nonferrous Metals Society of China, 2010, 20(6): 1046−1052.
[21] LOUE W R, SUERY M. Microstructural evolution during partial remelting of Al2Si7Mg alloys [J]. Materials Science and Engineering A, 1995, 203(1−2): 1−13.
[22] VOORHEES P W, HARDY S C. Ostwald ripening in a system with a high volume fraction of coarsening phase [J]. Metallurgical and Materials Transactions A, 1988, 19(11): 2713−2721.
[23] HU Geng-xiang, CAI Xun, RONG Yong-hua. Fundamentals of materials science [M]. Shanghai: Shanghai Jiao Tong University Press, 2015: 230−232. (in Chinese)
[24] LI Yuan-dong, CHEN Ti-jun, MA Ying, YAN Feng-yun, HAO Yuan. Microstructural characteristic and secondary solidification behavior of AZ91D alloy prepared by thixoforming [J]. Transactions of Nonferrous Metals Society of China, 2008, 18(1): 18−23.
[25] MULLINS W W, SEKERKA R F. Morphological stability of a partical growing by diffusion or heat flow [J]. Journal of Applied Physics, 1963, 34(2): 323−329.
[26] HITCHCOCK M, WANG Y, FAN Z. Secondary solidification behaviour of the Al−Si−Mg alloy prepared by the rheo-diecasting process [J]. Acta Materialia, 2007. 55(5): 1589−1598.
[27] BURDEN M H, HUNT J D. Cellular and dendritic growth [J]. Journal of Crystal Growth, 1974, 22(2): 109−116.
[28] HUNT J D, LU S Z. Numerical modeling of cellular /dendritic array growth: spacing and structure predictions [J]. Metall Mater Trans A, 1996, 27(3): 611−623.

6061 变形铝合金自孕育流变压铸过程中的凝固行为

李 明[1]，李元东[1,2]，郑宏强[1]，黄晓锋[1,2]，陈体军[1,2]，马 颖[1,2]

1. 兰州理工大学 省部共建有色金属先进加工与再利用国家重点实验室，兰州 730050；
2. 兰州理工大学 有色金属合金及加工教育部重点实验室，兰州 730050

摘 要：采用自孕育法制备 6061 变形铝合金半固态浆料，研究保温参数对自孕育流变压铸过程中凝固组织的影响，并结合 OM、SEM、EDS 及 EBSD 进一步分析流变压铸过程中的凝固行为。结果表明，保温过程只影响初生 α(Al)颗粒，而对 6061 合金薄壁件压铸过程中剩余液相的凝固组织影响不大。流变压铸过程中，型腔提供的较大冷却速率使剩余液相爆发形核，并经过稳定生长、失稳生长以及合并长大阶段最终形成二次凝固颗粒(α_2)。由于二次凝固过程中已经存在一次颗粒，剩余液相的溶质浓度较一次颗粒的高；因此，二次颗粒中 Mg 元素和 Si 元素的含量比一次颗粒中的高。

关键词：6061 变形铝合金；凝固行为；初生颗粒；二次颗粒；流变压铸

(Edited by Bing YANG)